Probabilistic Engineering Mechanics 71 (2023) 103410

Contents lists available at ScienceDirect

Probabilistic Engineering Mechanics

journal homepage: www.elsevier.com/locate/probengmech

A Wiener path integral technique for determining the stochastic response of nonlinear oscillators with fractional derivative elements: A constrained variational formulation with free boundaries

Yuanjin Zhang [a], Ioannis A. Kougioumtzoglou [b,*], Fan Kong [c]

[a] School of Safety Science and Emergency Management, Wuhan University of Technology, 122 Luoshi Road, Wuhan, 430070, China
[b] Department of Civil Engineering and Engineering Mechanics, Columbia University, 500 West 120th Street, New York, 10027, NY, USA
[c] School of Civil Engineering, Hefei University of Technology, Hefei, 230009, China

ARTICLE INFO

Keywords:
Nonlinear system
Fractional derivative
Stochastic dynamics
Path integral
Variational principles

ABSTRACT

A technique based on the concept of Wiener path integral (WPI) is developed for determining approximately the joint response probability density function (PDF) of nonlinear oscillators endowed with fractional derivative elements. Specifically, first, the dependence of the state of the system on its history due to the fractional derivative terms is accounted for, alternatively, by augmenting the response vector and by considering additional auxiliary state variables and equations. In this regard, the original single-degree-of-freedom (SDOF) nonlinear system with fractional derivative terms is cast, equivalently, into a multi-degree-of-freedom (MDOF) nonlinear system involving integer-order derivatives only. From a mathematics perspective, the equations of motion referring to the latter can be interpreted as constrained. Second, to circumvent the challenge of increased dimensionality of the problem due to the augmentation of the response vector, a WPI formulation with mixed fixed/free boundary conditions is developed for determining directly any lower-dimensional joint PDF corresponding to a subset only of the response vector components. This can be construed as an approximation-free dimension reduction approach that renders the associated computational cost independent of the total number of stochastic dimensions of the problem. Thus, the original SDOF oscillator joint PDF corresponding to the response displacement and velocity is determined efficiently, while circumventing the computationally challenging task of treating directly equations of motion involving fractional derivatives. Two illustrative numerical examples are considered for demonstrating the reliability of the developed technique. These pertain to a nonlinear Duffing and a nonlinear vibro-impact oscillators with fractional derivative elements subjected to combined stochastic and deterministic periodic loading. Note that alternative standard approximate techniques, such as statistical linearization, need to be significantly modified and extended to account for such cases of combined loading. Remarkably, it is shown herein that the WPI technique exhibits the additional advantage of treating such types of excitation in a straightforward manner without the need for any ad hoc modifications. Comparisons with pertinent Monte Carlo simulation data are included as well.

1. Introduction

Addressing the challenge of uncertainty quantification in engineering dynamics relates to the development of analytical and numerical methodologies for determining response and reliability statistics of complex systems. Indicative techniques include moments equations, statistical linearization, stochastic averaging, perturbation approaches, discrete versions of the Chapman–Kolmogorov equation, Fokker–Planck equation solution schemes, probability density evolution methods, as well as sparse representations and polynomial chaos expansions; see [1–7] for a broad perspective.

Further, relying on the mathematical tool of Wiener path integral (WPI) [8,9], Kougioumtzoglou and co-workers have recently developed a solution technique in stochastic engineering dynamics that exhibits both high accuracy and low computational cost. The basic concept of the technique relates to treating, formally, the system response joint transition probability density function (PDF) as a functional integral over the space of all possible paths connecting the initial and the final states of the response vector. Notably, this functional integral is rarely amenable to analytical evaluation. Thus, an approximate calculation is pursued by considering, ordinarily, the contribution only of the path with the maximum probability of occurrence. This is known as the

* Corresponding author.
E-mail address: ikougioum@columbia.edu (I.A. Kougioumtzoglou).

https://doi.org/10.1016/j.probengmech.2022.103410
Received 28 June 2022; Accepted 27 December 2022
Available online 2 January 2023

most probable path and corresponds to an extremum of the functional integrand. In this regard, the most probable path is determined by solving a functional minimization problem that takes the form of a deterministic boundary value problem (BVP) [10,11].

Remarkably, the WPI technique is capable of determining the joint response transition PDF of multi-degree-of-freedom (MDOF) systems exhibiting diverse nonlinear/hysteretic behaviors and excited by non-white/non-Gaussian stochastic processes (e.g., [12–14]). Further, it has been shown that the computational cost associated with a brute-force numerical implementation of the technique can be drastically reduced by employing sparse representations for the system response PDF in conjunction with compressive sampling schemes and group sparsity concepts [15,16]. Furthermore, high-dimensional systems can be readily treated by relying on a variational formulation with mixed fixed/free boundary conditions that renders the computational cost independent of the total number of stochastic dimensions [17].

Nevertheless, note that classical continuum (or discretized) mechanics theories have been traditionally used for modeling the system equations of motion. In this regard, the generalization of the aforementioned solution approaches to treat systems exhibiting time- and space-localized behaviors, described by operators based on wavelets and/or non-integer order derivatives, can be a rather challenging task (e.g., [18–20]). In fact, the need for more accurate media behavior modeling has led recently to advanced mathematical tools such as fractional calculus (e.g., [21–23]). Fractional calculus can be construed as a generalization of ordinary calculus, and as such provides with enhanced modeling capabilities. In this context, it has been successfully employed in theoretical and applied mechanics for developing non-local continuum mechanics theories (e.g., [24,25]), as well as for modeling viscoelastic materials (e.g., [26]).

Several methodologies have been developed over the past few years, with varying degrees of success, for determining the stochastic response of nonlinear oscillators endowed with fractional derivative elements. Indicatively, a large number of research efforts pertain to extensions of the well-established techniques of stochastic averaging and statistical linearization to account for fractional derivative modeling (e.g., [27–30]). However, a stochastic averaging solution treatment is associated typically with significant approximations, whereas the standard formulation of statistical linearization yields second-order response statistics only. Further, a WPI-based technique was proposed in [31] for treating nonlinear systems with fractional derivative elements subject to Gaussian white noise excitation. Specifically, resorting to a variational principle led to a functional minimization problem that was cast in the form of a deterministic BVP involving Euler–Lagrange equations with fractional derivative terms. Obviously, addressing the resulting fractional BVP has its own theoretical and methodological merit. Nevertheless, its solution is associated with significant challenges both from an analytical treatment and a computational cost perspectives.

In this paper, to circumvent solving a computationally cumbersome deterministic BVP with fractional derivative terms [31], an alternative formulation of the WPI technique is pursued. Specifically, relying on a transformation proposed in [32] and considering additional auxiliary state variables, the original single-degree-of-freedom (SDOF) nonlinear system endowed with fractional derivative elements is cast, equivalently, into a MDOF nonlinear system involving integer-order derivatives only. Thus, it can be argued that the complexity of the original equation of motion is reduced. However, note that the dimensionality of the problem increases significantly due to the augmentation of the response vector. To bypass this challenge, the WPI variational formulation with mixed fixed/free boundary conditions, which was developed originally in [17], is employed and extended herein to treat the resulting constrained functional minimization problem. In this regard, the developed technique is capable of determining directly any lower-dimensional joint PDF corresponding to a subset only of the response vector components. Note that this is done in an a priori manner; that is, without computing the multi-dimensional joint PDF first and marginalizing afterwards. In fact, due to this a priori marginalization the associated computational cost of the technique becomes independent of the total number of stochastic dimensions of the problem. Thus, the curse of dimensionality in stochastic dynamics is circumvented and the original SDOF oscillator response joint PDF can be determined efficiently.

Two illustrative numerical examples are considered for demonstrating the reliability of the developed technique. These pertain to a nonlinear Duffing and a nonlinear vibro-impact oscillators with fractional derivative elements subjected to combined loading. In particular, the applied excitation comprises a white noise and a deterministic harmonic components. Interestingly, alternative standard approximate techniques, such as stochastic averaging and statistical linearization, need to be significantly modified and extended to account for such cases of combined stochastic and deterministic periodic loading (e.g., [33–36]). In this regard, it is shown herein that such types of combined loading, for which the purely stochastic excitation can be construed as a special case, can be treated by the WPI technique in a straightforward manner without the need for any ad hoc modifications of the original formulation of the technique. Comparisons with pertinent Monte Carlo simulation (MCS) data are included as well.

2. Mathematical formulation

2.1. Governing equation of motion

A SDOF nonlinear oscillator endowed with fractional derivative elements is considered next subjected both to stochastic loading and to a deterministic harmonic excitation component. Its equation of motion takes the form

$$\ddot{x} + C_\alpha D^\alpha(x) + g(x, \dot{x}) = w(t) + F_1 \sin(\omega_1 t) \tag{1}$$

where x represents the nonlinear system response displacement, and a dot over a variable denotes differentiation with respect to time t; $g(x, \dot{x})$ is an arbitrary nonlinear function; $w(t)$ is a Gaussian zero-mean white noise excitation process with a constant power spectrum value equal to S_0; F_1 and ω_1 represent the amplitude and frequency of the harmonic excitation component, respectively. Further, $D^\alpha(x)$ denotes an α-order Caputo fractional derivative defined as

$$D^\alpha(x) = \frac{1}{\Gamma(1-\alpha)} \int_0^t \frac{\dot{x}(\tau)}{(t-\tau)^\alpha} \mathrm{d}\tau, \quad 0 < \alpha < 1 \tag{2}$$

where $\Gamma(\cdot)$ is the Gamma function given by

$$\Gamma(\alpha) = \int_0^\infty e^{-\kappa} \kappa^{\alpha-1} d\kappa \tag{3}$$

and C_α represents a coefficient associated with the fractional derivative term.

Next, following [32,37], Eq. (1) is recast, equivalently, in a form containing integer-order derivatives only. Specifically, employing Eq. (3) and the relationship $\Gamma(\alpha)\Gamma(1-\alpha) = \pi/sin(\alpha\pi)$, and setting $\kappa = (t-\tau)y^2$, Eq. (2) becomes

$$D^\alpha(x) = \mu \int_0^\infty y^{2\alpha-1} \left(\int_0^t e^{-(t-\tau)y^2} \dot{x}(\tau) d\tau \right) dy \tag{4}$$

where $\mu = 2sin(\pi\alpha)/\pi$. Further, note that the expression

$$u_y(t) = \int_0^t e^{-(t-\tau)y^2} \dot{x}(\tau) d\tau \tag{5}$$

for $u_y(t = 0) = 0$ can be construed as the solution of the differential equation

$$\dot{u}_y(t) + y^2 u_y(t) = \dot{x}(t); \qquad u_y(0) = 0 \tag{6}$$

Clearly, taking into account Eq. (5), Eq. (4) can be written as

$$D^\alpha(x) = \mu \int_0^\infty u_y(t) y^{2\alpha-1} dy \tag{7}$$

or, approximately, as

$$D^{\alpha}(x) \approx \mu \sum_{j=1}^{\infty} u_{y,j}(t) y_j^{2\alpha-1} \Delta y \tag{8}$$

where $y_j = j\Delta y$. Furthermore, considering Eqs. (6) and (8), Eq. (1) can be cast in the form

$$\begin{aligned} &\ddot{x}(t) + C_{\alpha}\mu \sum_{j=1}^{\infty} u_{y,j}(t) y_j^{2\alpha-1} \Delta y + g(x,\dot{x}) = w(t) + F_1 \sin(\omega_1 t); \\ &\dot{u}_{y,j}(t) + y_j^2 u_{y,j}(t) = \dot{x}(t), \quad j = 1,2,\ldots,\infty \end{aligned} \tag{9}$$

Obviously, for numerical applications the summation in Eq. (9) is truncated after n terms. Alternatively, Eq. (9) can be expressed in the matrix form

$$\mathbf{M}\ddot{\mathbf{x}} + \mathbf{h}(\mathbf{x},\dot{\mathbf{x}},t) = \mathbf{w}(t) \tag{10}$$

where $\mathbf{x} = [x(t), \mathbf{u}_y^T]^T$ with $\mathbf{u}_y = [u_{y,1}(t),\ldots,u_{y,n}(t)]^T$, $\mathbf{w}(t) = [w(t),0,\ldots,0]^T$,

$$\mathbf{M} = \begin{bmatrix} 1 & 0 & \cdots & 0 \\ 0 & 0 & \cdots & 0 \\ \vdots & \vdots & \ddots & \vdots \\ 0 & 0 & \cdots & 0 \end{bmatrix} \tag{11}$$

and

$$\mathbf{h}(\mathbf{x},\dot{\mathbf{x}},t) = \begin{bmatrix} C_{\alpha}\mu \sum_{j=1}^{n} u_{y,j}(t) y_j^{2\alpha-1} \Delta y + g(x,\dot{x}) - F_1 \sin(\omega_1 t) \\ \mathbf{f}_{n\times 1}(\mathbf{x},\dot{\mathbf{x}}) \end{bmatrix} \tag{12}$$

where

$$\mathbf{f}_{n\times 1}(\mathbf{x},\dot{\mathbf{x}}) = \begin{bmatrix} \dot{u}_{y,1}(t) + y_1^2 u_{y,1}(t) - \dot{x}(t) \\ \vdots \\ \dot{u}_{y,n}(t) + y_j^2 u_{y,n}(t) - \dot{x}(t) \end{bmatrix} \tag{13}$$

It is readily seen that the original SDOF nonlinear system endowed with fractional derivative elements and governed by Eq. (1) has been recast into the MDOF nonlinear system of Eq. (10) involving integer-order derivatives only. Thus, it can be argued that the complexity of the original equation has been reduced. Note, however, that the dimensionality of the problem has increased significantly due to the augmentation of the response vector. Of course, this does not pose any considerable computational challenges for the special case of linear systems, i.e., $g(x,\dot{x})$ in Eq. (1) is a linear function of x and $\dot{x}$. Indeed, as shown in [32], standard linear random vibration theory tools can be employed for determining the MDOF system response statistics efficiently, even in closed-form for some cases; see also [2] for a broader perspective.

Nevertheless, determining response statistics for the general case of the nonlinear MDOF system in Eq. (10), accurately and in a computationally efficient manner, has been a persistent challenge in the field of stochastic engineering dynamics (e.g., [4]). In the following, the WPI solution technique developed recently by Kougioumtzoglou and co-workers (e.g., [14,17]) is extended and applied herein to treat the nonlinear system of Eq. (10), and to determine its response joint PDF $p(x,\dot{x})$.

2.2. Wiener path integral technique formulation

It is seen that Eq. (10) describing the motion of the nonlinear MDOF system involves an $(n+1)\times 1$ excitation vector $\mathbf{w}(t)$ with n zero entries. In this regard, the resulting constant matrix $\mathbf{D}$, where $E[\mathbf{w}(t)\mathbf{w}(t+\tau)^T] = \mathbf{D}\delta(\tau)$, becomes singular. Thus, the special WPI solution formulation developed in [14] to account for singular $\mathbf{D}$ matrices is adapted next to treat Eq. (10).

Specifically, the singularity of $\mathbf{D}$ is addressed by interpreting Eq. (10) as a set of two coupled subsystems. The first refers to the first row of Eq. (10) corresponding to the excitation $w(t)$. The second pertains to the vector $\mathbf{f}_{n\times 1}$ in Eq. (13) corresponding to the zero entries of $\mathbf{w}(t)$. In other words, it can be argued that the motion of the MDOF dynamical system is governed by the first subsystem constrained, however, by the second subsystem of equations. Based on the above rationale, it was shown in [14] that the joint response transition PDF of such systems can be represented as a functional integral over the space of all paths satisfying the constraint equations.

In particular, referring to the system of Eq. (10), the joint response transition PDF $p(x_f,\dot{x}_f,\mathbf{u}_{yf},t_f|x_i,\dot{x}_i,\mathbf{u}_{yi},\ t_i)$ starting from the initial state $(x_i,\dot{x}_i,\mathbf{u}_{yi},t_i)$ and reaching the final state $(x_f,\dot{x}_f,\mathbf{u}_{yf},t_f)$ takes the form of the functional integral

$$p(x_f,\dot{x}_f,\mathbf{u}_{yf},t_f|x_i,\dot{x}_i,\mathbf{u}_{yi},t_i) = \int_{C\{x_i,\dot{x}_i,\mathbf{u}_{yi},t_i;x_f,\dot{x}_f,\mathbf{u}_{yf},t_f|\mathbf{f}_{n\times 1}=0\}} \exp\left(-\int_{t_i}^{t_f} L(x,\dot{x},\ddot{x},\mathbf{u}_y)dt\right) d\mathbf{x}(t) \tag{14}$$

where $L(x,\dot{x},\ddot{x},\mathbf{u}_y)$ denotes the Lagrangian functional given by

$$L(x,\dot{x},\ddot{x},\mathbf{u}_y) = \frac{[\ddot{x}(t) + C_{\alpha}\mu \sum_{j=1}^{n} u_{y,j}(t) y_j^{2\alpha-1} \Delta y + g(x,\dot{x}) - F_1 \sin(\omega_1 t)]^2}{4\pi S_0} \tag{15}$$

In Eq. (14), $d\mathbf{x}(t)$ represents a functional measure, and $C\{x_i,\dot{x}_i,\mathbf{u}_{yi},t_i;$ $x_f,\dot{x}_f,\ \mathbf{u}_{yf},t_f|\mathbf{f}_{n\times 1} = 0\}$ denotes the set of all paths with initial state $(x_i,\dot{x}_i,\mathbf{u}_{yi},t_i)$ and final state $(x_f,\dot{x}_f,\mathbf{u}_{yf},t_f)$ satisfying the constraint $\mathbf{f}_{n\times 1} = 0$.

Note that the joint PDF in Eq. (14) refers to the augmented $(n+1)\times 1$ response vector $\mathbf{x}$. However, from a practical point of view, the primary objective relates to determining the joint PDF of the response displacement x and velocity $\dot{x}$ corresponding to the original oscillator of Eq. (1). In other words, it can be argued that knowledge of the joint PDF corresponding to vector $\mathbf{u}_y$ is of limited practical value. Indeed, $\mathbf{u}_y$ constitutes a vector of auxiliary variables used to model the dependence of the state of the oscillator on its history due to the fractional derivative term.

In this regard, the WPI variational formulation with mixed fixed/free boundary conditions, which was developed originally in [17], is employed and extended herein to account for constrained problems such as the one shown in Eq. (14). Specifically, considering the response vector $\mathbf{x}$, the technique is capable of determining directly any lower-dimensional joint PDF corresponding to a subset only of the components of the vector $\mathbf{x}$. Note that this is done in an a priori manner; that is, without computing the complete $(n+2)$-dimensional joint PDF first and marginalizing afterwards. Further, as demonstrated in [17] and remarked also in Section 2.4, due to this a priori marginalization the computational cost of the technique becomes independent of the total number of stochastic dimensions of the problem. Thus, the curse of dimensionality in stochastic dynamics is circumvented and the joint PDF $p(x,\dot{x})$ can be determined efficiently.

In particular, the transition PDF of Eq. (14) becomes

$$p(x_f,\dot{x}_f,t_f|x_i,\dot{x}_i,\mathbf{u}_{yi},t_i) = \int_{C\{x_i,\dot{x}_i,\mathbf{u}_{yi},t_i;x_f,\dot{x}_f,t_f|\mathbf{f}_{n\times 1}=0\}} \exp\left(-\int_{t_i}^{t_f} L(x,\dot{x},\ddot{x},\mathbf{u}_y)dt\right) d\mathbf{x}(t) \tag{16}$$

Note that the coordinates $\mathbf{u}_y$ at t_f are considered free; see also [17] for more details.

2.3. Constrained variational problem and system response joint PDF determination

Evaluating analytically the functional integral of Eq. (16) is, in general, an impossible task. To address this challenge, approximate approaches are typically employed in the literature such as the most probable path approximation (e.g., [11]). It is remarked that the most probable path approximation has exhibited a quite high degree of accuracy in various diverse engineering mechanics applications (e.g., [10,38,39]). In fact, as proved in [40], for the case of linear systems the most probable path approximation yields the exact joint response PDF.

In particular, note that the largest contribution to the functional integral of Eq. (16) relates to the trajectory $\mathbf{x}_c(t) = [x_c(t), \mathbf{u}_{y,c}^T]^T$ for which the integral in the exponential becomes as small as possible. This leads to the constrained variational (functional minimization) problem

$$\begin{aligned} &\text{minimize} \quad J(\mathbf{x}) = \int_{t_i}^{t_f} L(x, \dot{x}, \ddot{x}, \mathbf{u}_y) dt \\ &\text{subject to} \quad \mathbf{f}_{n\times 1} = 0 \end{aligned} \tag{17}$$

Next, the most probable path $\mathbf{x}_c(t)$ satisfying Eq. (17) can be used in conjunction with Eq. (16) for determining approximately the system response joint transition PDF as

$$p(x_f, \dot{x}_f, t_f | x_i, \dot{x}_i, \mathbf{u}_{yi}, t_i) \approx C \exp\left(-\int_{t_i}^{t_f} L(x_c, \dot{x}_c, \ddot{x}_c, \mathbf{u}_{y,c}) dt\right) \tag{18}$$

where C is a normalization constant determined by

$$\int_{-\infty}^{+\infty}\int_{-\infty}^{+\infty} p(x_f, \dot{x}_f, t_f | x_i, \dot{x}_i, \mathbf{u}_{yi}, t_i) dx_f d\dot{x}_f = 1 \tag{19}$$

Further, the constrained variational problem of Eq. (17) can be cast in the form of an unconstrained problem by employing an approach based on Lagrange multipliers (e.g., [41]). Specifically, defining the auxiliary Lagrangian functional

$$L^*(x, \dot{x}, \ddot{x}, \mathbf{u}_y) = L(x, \dot{x}, \ddot{x}, \mathbf{u}_y) + \lambda(t)^T \mathbf{f}_{n\times 1} \tag{20}$$

Eq. (17) becomes

$$\text{minimize} \quad J^*(\mathbf{x}) = \int_{t_i}^{t_f} L^*(x, \dot{x}, \ddot{x}, \mathbf{u}_y) dt \tag{21}$$

where $\lambda(t)$ in Eq. (20) denotes the n-dimensional vector of the Lagrange multiplier functions. Furthermore, the most probable path $\mathbf{x}_c(t)$ that minimizes $J^*(\mathbf{x})$ is an extremal of the functional $J^*(\mathbf{x})$. According to the fundamental theorem of calculus of variations [42], an extremal can be evaluated by enforcing the necessary condition that the first variation of the functional vanishes, i.e.,

$$\delta J^*(\mathbf{x}) = 0 \tag{22}$$

Applying Eq. (22) in conjunction with fixed boundary conditions for $(x, \dot{x}, \mathbf{u}_y)$ at t_i, and fixed conditions for $(x, \dot{x})$ and free conditions for $\mathbf{u}_y$ at t_f, yields the Euler–Lagrange equations (e.g., [17])

$$\frac{\partial L^*}{\partial x_j} - \frac{\partial}{\partial t}\frac{\partial L^*}{\partial \dot{x}_j} + \frac{\partial^2}{\partial t^2}\frac{\partial L^*}{\partial \ddot{x}_j} = 0, \ j = 1, 2, \dots, n+1 \tag{23}$$

where x_j denotes the j-th component of the vector $\mathbf{x} = [x(t), \mathbf{u}_y^T]^T$. Eq. (23) is subjected to the boundary conditions

$$\begin{aligned} &x(t_i) = x_i, \qquad \dot{x}(t_i) = \dot{x}_i, \\ &u_{y,j}(t_i) = u_{yi,j}, \quad j = 1, 2, \dots, n \end{aligned} \tag{24}$$

$$x(t_f) = x_f, \qquad \dot{x}(t_f) = \dot{x}_f \tag{25}$$

$$\left[\frac{\partial L^*}{\partial \dot{u}_{y,j}}\right]_{t=t_f} = 0, \quad j = 1, 2, \dots, n \tag{26}$$

Eqs. (23)–(26) need to be solved in conjunction with the n constraint equations $\mathbf{f}_{n\times 1} = 0$ for determining both $\mathbf{x}_c(t)$ and the Lagrange multipliers $\lambda(t)$. In this regard, note that $\dot{u}_{y,j}(t_i) = \dot{x}_i - y_j^2 u_{yi,j}$, for $j = 1, 2, \dots, n$, reflecting the constraint relationship at t_i. The interested reader is also directed to the Appendix for a detailed derivation of Eqs. (23)–(26).

2.4. Computational aspects

Clearly, solution of the functional minimization problem of Eq. (17), or equivalently of the Euler–Lagrange Eqs. (23)–(26), yields the most probable path $\mathbf{x}_c(t)$ to be substituted into Eq. (18) for determining a specific point of the response PDF. In this regard, it is readily seen that a brute-force approach for computing the complete 2-dimensional transition PDF $p(x_f, \dot{x}_f, t_f | x_i, \dot{x}_i, \mathbf{u}_{yi}, t_i)$ at time instant t_f dictates, first, the discretization of the $(x_f, \dot{x}_f)$ domain into N^2 points, where N is the number of points in each dimension, and second, the numerical solution of N^2 problems of the form of Eq. (17); see also [17] for more details.

The aforementioned approach demonstrates the significant advantage, in terms of computational efficiency, of the herein extended WPI formulation with mixed fixed/free boundaries that marginalizes the system response joint PDF in an a priori manner. To elaborate further, applying an alternative standard WPI formulation involving only fixed boundaries dictates the PDF representation of Eq. (14) corresponding to the augmented response vector $[x_f, \mathbf{u}_{yf}^T]^T$. In this regard, determining the $(n+2)$-dimensional transition PDF $p(x_f, \dot{x}_f, \mathbf{u}_{yf}, t_f | x_i, \dot{x}_i, \mathbf{u}_{yi}, t_i)$ at time instant t_f relates, first, to discretizing the $(x_f, \dot{x}_f, \mathbf{u}_{yf})$ domain into $N^{(2+n)}$ points, and second, to solving $N^{(2+n)}$ problems of the form of Eq. (23), but with fixed boundary conditions at both t_i and t_f for the state variables $(x, \dot{x}, \mathbf{u}_y)$. Obviously, this yields a prohibitive computational cost taking into account that $n \sim O(10^2)$ as shown in [32].

In the ensuing analysis and numerical examples a Rayleigh–Ritz solution approach is employed for determining the most probable path $\mathbf{x}_c(t)$ (e.g., [10,11]). Specifically, $\mathbf{x}_c(t)$ is approximated by

$$\mathbf{x}_c(t) \approx \boldsymbol{\psi}(t) + \mathbf{R}\mathbf{h}(t) \tag{27}$$

where $\mathbf{h}(t) = [h_l(t)]_{m\times 1}$ denotes a vector of m trial functions vanishing at the boundaries, i.e., $\mathbf{h}(t_i) = \mathbf{h}(t_f) = 0$; $\mathbf{R} \in \mathbb{R}^{(n+1)\times m}$ is a coefficient matrix to be determined; and $\boldsymbol{\psi}(t) = [\psi_q(t)]_{(n+1)\times 1}$ is an appropriately chosen vector function satisfying the boundary conditions. In particular, the Hermite interpolating polynomials

$$\psi_q(t) = \sum_{k=0}^{3} a_{q,k} t^k, \qquad q = 1, 2, \dots, n, n+1 \tag{28}$$

are employed. Further, the trial functions vanishing at the boundaries take the form

$$h_l(t) = (t - t_i)^2 (t - t_f)^2 P_l(t) \tag{29}$$

where $P_l(t)$ denote the shifted Legendre polynomials given by the recursive formula

$$P_{l+1}(t) = \frac{2l+1}{l+1} P_1(t) P_l(t) - \frac{l}{l+1} P_{l-1}(t), \quad l = 1, 2, \dots \tag{30}$$

with $P_0(t) = 1$ and $P_1(t) = (2t - t_i - t_f)/(t_f - t_i)$.

Obviously, the adoption of the Rayleigh–Ritz solution approach simplifies the constrained variational (functional minimization) problem of Eq. (17) to an ordinary minimization problem of a function that depends on a finite number of variables [43]. That is, Eq. (17) becomes

$$\text{minimize} \quad J(\mathbf{R}) \tag{31}$$

$$\text{subject to} \quad \mathbf{f}_{n\times 1}(\mathbf{R}) = 0 \tag{32}$$

Notably, the fact that the constraint equations $\mathbf{f}_{n\times 1} = 0$ are linear facilitates a computationally efficient numerical solution of Eqs. (31)–(32) by employing the nullspace of the constraint equations; see also [14] for more details.

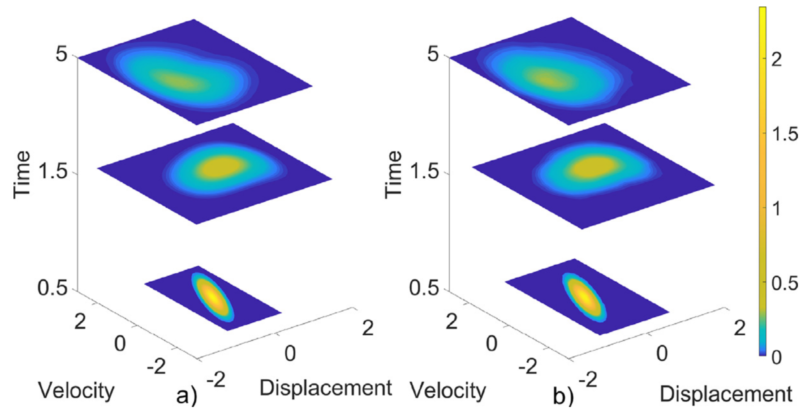

Fig. 1. Joint response PDF $p(x,\dot{x})$ at indicative time instants $t = 0.5$, 1.5 and 5 s of a Duffing nonlinear oscillator with a fractional derivative element: (a) WPI technique; (b) MCS data (10,000 realizations).

3. Numerical examples

In this section, two illustrative numerical examples are considered for demonstrating the reliability of the developed technique. These pertain to a nonlinear Duffing and a nonlinear vibro-impact oscillators with fractional derivative elements governed by Eq. (1) and starting from rest. The joint response PDF estimates obtained by the herein developed WPI technique are compared with MCS-based estimates obtained by numerically solving Eq. (1) and by conducting a statistical analysis on the response time-histories (10,000 realizations). To this aim, the L_1-algorithm [44] is utilized for numerically integrating Eq. (1).

Further, $n \sim O(10^2)$ as shown in [32]. In this regard, to reduce the number n of additional state-variables $\mathbf{u}_y$ required in the transformed system of Eq. (9), the Laguerre formula is employed next for approximating the integral of Eq. (7) [37]. Specifically, considering Eqs. (7) and (8) yields

$$\begin{aligned} D^{\alpha}(x) &= \mu \int_0^{\infty} u_y(t) y^{2\alpha-1} dy \approx \mu \sum_{j=1}^{n} u_{y,j}(t) y_j^{2\alpha-1} \Delta y \\ &\approx \mu \sum_{j=1}^{n_L} k_j e^{y_j} y_j^{2\alpha-1} u_{y,j}(t) \end{aligned} \quad (33)$$

where k_j and $y_j, j = 1,2,\ldots,n_L$ denote the Laguerre weights and node points, respectively. As shown in [37], $n_L \sim O(10^1)$ that is approximately an order of magnitude smaller than n.

3.1. Nonlinear duffing oscillator

Consider a Duffing nonlinear oscillator with a fractional derivative element, whose dynamics is governed by Eq. (1) with

$$g(x,\dot{x}) = \omega_0^2 x + \varepsilon \omega_0^2 x^3 \quad (34)$$

In Eq. (34), ω_0 denotes the natural frequency of the corresponding linear oscillator (i.e., for $\varepsilon = 0$), and the parameter $\varepsilon > 0$ controls the magnitude of the nonlinearity. In the following, the parameter values used are $S_0 = 1/(2\pi), C_\alpha = 1, \alpha = 0.6, \omega_0 = 1, \varepsilon = 1, F_1 = 1.5, \omega_1 = 1$, and $n_L = 5$.

Further, employing the herein developed WPI technique described in Section 2.3, with free boundaries at t_f for the state variables $\mathbf{u}_y$, yields the joint response PDF $p(x,\dot{x})$ shown in Fig. 1a for three arbitrary time instants, i.e., $t = 0.5$, 1.5 and 5 s. Comparisons with MCS-based estimates in Fig. 1b demonstrate a satisfactory degree of accuracy. Furthermore, the marginal response displacement and velocity PDFs are plotted in Figs. 2 and 3, respectively, for $t = 0.5$ s, 1.5 s and 5 s. Clearly, the accuracy degree exhibited by the WPI technique based on comparisons with MCS data is quite high, even for the herein considered challenging case of combined loading. In this regard, not only the technique is capable of treating such excitation types in a straightforward manner without the need for any ad hoc modifications, but it also succeeds in capturing the strongly time-variant behavior of the response PDF due to the sinusoidal excitation component.

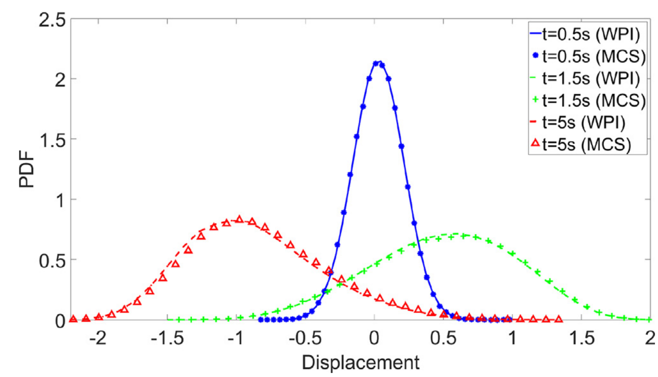

Fig. 2. Response displacement PDF of a Duffing nonlinear oscillator with a fractional derivative element at indicative time instants $t = 0.5, 1.5$ and 5 s; comparisons with MCS data (10,000 realizations).

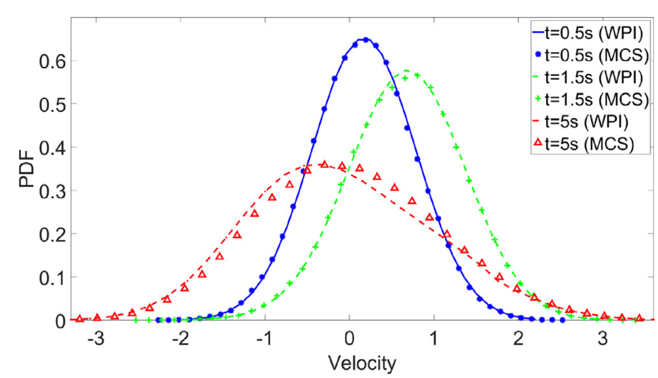

Fig. 3. Response velocity PDF of a Duffing nonlinear oscillator with a fractional derivative element at indicative time instants $t = 0.5, 1.5$ and 5 s; comparisons with MCS data (10,000 realizations).

3.2. Nonlinear vibro-impact oscillator

Consider a nonlinear vibro-impact oscillator with a fractional derivative element. Its equation of motion is given by Eq. (1) with

$$g(x,\dot{x}) = \omega_0^2 x + \eta h(x) \quad (35)$$

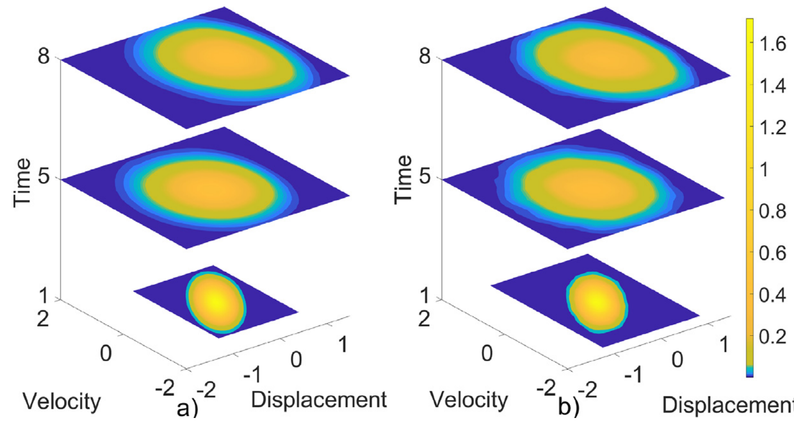

Fig. 4. Joint response PDF $p(x, \dot{x})$ at indicative time instants $t = 1$, 5 and 8 s of a vibro-impact nonlinear oscillator with a fractional derivative element: (a) WPI technique; (b) MCS data (10,000 realizations).

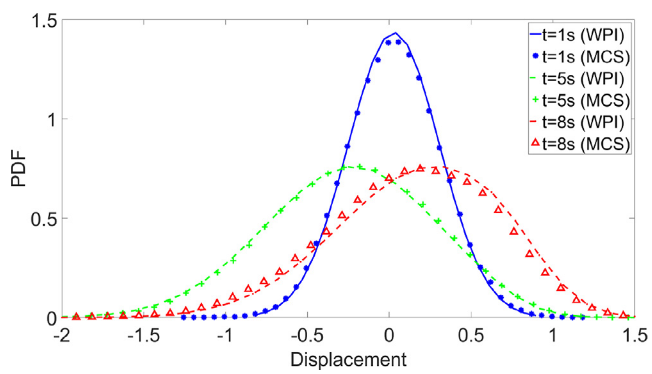

Fig. 5. Response displacement PDF of a vibro-impact nonlinear oscillator with a fractional derivative element at indicative time instants $t = 1, 5$ and 8 s; comparisons with MCS data (10,000 realizations).

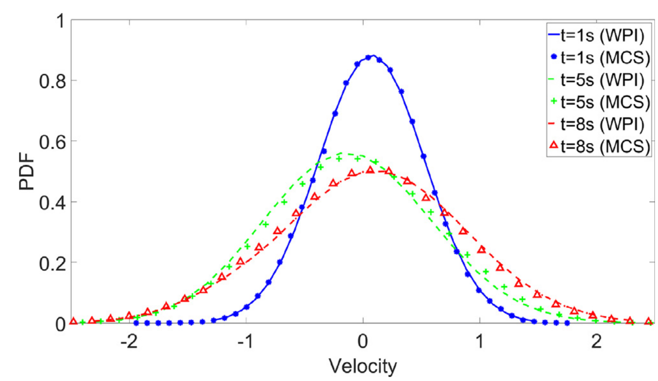

Fig. 6. Response velocity PDF of a vibro-impact nonlinear oscillator with a fractional derivative element at indicative time instants $t = 1, 5$ and 8 s; comparisons with MCS data (10,000 realizations).

where

$$h(x) = \begin{cases} (x-a)^{3/2} & \text{if } x \geq a \\ 0 & \text{otherwise} \end{cases} \quad (36)$$

In Eqs. (35)–(36), ω_0 denotes the natural frequency of the corresponding linear oscillator (i.e., for $\eta = 0$); the parameter η controls the nonlinearity magnitude; and a represents the displacement bound. The interested reader is also directed to the review paper [45] for more details and for a broader perspective. In the following, the parameter values $S_0 = 0.0637, C_\alpha = 1, \alpha = 0.3, \omega_0 = 1, \eta = 4, a = 0.5, F_1 = 0.2, \omega_1 = 1$, and $n_L = 4$ are used.

Similarly to the example in Section 3.1, applying the WPI technique of Section 2.3 and solving the constrained optimization problem described by Eqs. (31)–(32) yields the most probable path. This is substituted in Eq. (16) for evaluating the joint response PDF $p(x, \dot{x})$. This is plotted in Fig. 4 for indicative time instants $t = 1, 5$, and 8 s and compared with pertinent MCS data (10,000 realizations). Further, the corresponding marginal response displacement and velocity PDFs are plotted in Figs. 5 and 6, respectively, for $t = 1, 5$, and 8 s. It is seen that the WPI technique exhibits a satisfactory accuracy degree, even for the highly asymmetric displacement PDF shape at $t = 8$ s.

4. Concluding remarks

In this paper, a WPI technique has been developed for determining the joint response PDF of nonlinear oscillators with fractional derivative elements. In this regard, relying on a transformation proposed in [32], the original SDOF nonlinear system with fractional derivative terms has been cast into a MDOF nonlinear system involving integer-order derivatives only. In particular, the dependence of the state of the oscillator on its history due to the fractional derivative terms has been accounted for by augmenting the response vector and by considering additional auxiliary state variables and equations.

Further, the MDOF system equations of motion have been treated as a set of two coupled subsystems. The rationale relates to the interpretation that the first subsystem corresponding to the applied excitation governs the motion of the MDOF system, which is constrained, however, by the second subsystem of equations. Furthermore, to address the challenge of increased dimensionality of the MDOF system, a WPI formulation with mixed fixed/free boundary conditions has been developed for determining directly any lower-dimensional joint PDF corresponding to a subset only of the response vector components. Note that this is done in an a priori manner; that is, without computing the complete multi-dimensional joint PDF first and marginalizing afterwards. In fact, due to this a priori marginalization the associated computational cost becomes independent of the total number of stochastic dimensions of the problem. Thus, the original SDOF oscillator joint PDF corresponding to the response displacement and velocity has been determined efficiently, while circumventing the analytically and computationally challenging task of treating directly equations of motion involving fractional derivatives. Notably, the developed technique can be construed also as an extension of the concepts and results in [17] to account for equations of motion with constraints.

Two illustrative numerical examples have been considered for demonstrating the reliability of the developed technique, pertaining to a nonlinear Duffing and a nonlinear vibro-impact oscillators with fractional derivative elements subjected to combined stochastic and deterministic periodic loading. Remarkably, compared to alternative standard approximate techniques that need to be significantly modified and extended to account for such cases of combined loading (e.g., [33–36]), it has been shown herein that the WPI technique can treat such types of excitation in a straightforward manner without the need for any ad hoc modifications. Comparisons with pertinent MCS data have demonstrated a quite high accuracy degree of the WPI technique.

Declaration of competing interest

The authors declare that they have no known competing financial interests or personal relationships that could have appeared to influence the work reported in this paper.

Acknowledgment

Y. Zhang acknowledges the support by the Natural Science Fund of Hubei province, China (Grant no. 2021CFB017). I.A. Kougioumtzoglou gratefully acknowledges the support through his CAREER award by the CMMI Division of the National Science Foundation, USA (Award no. 1748537). F. Kong acknowledges the support by the National Natural Science Foundation of China (Grant no. 52078399).

Appendix

In this Appendix, additional details are provided regarding the derivation of the Euler–Lagrange equations shown in Eq. (23) and the associated mixed fixed/free boundary conditions of Eqs. (24)–(25). Specifically, considering Eq. (21), the first variation of the functional $J^*(\mathbf{x})$ becomes

$$\delta J^*(\mathbf{x}) = \int_{t_i}^{t_f} \left[L^*\left(\mathbf{x}+\delta\mathbf{x}, \dot{\mathbf{x}}+\delta\dot{\mathbf{x}}, \ddot{\mathbf{x}}+\delta\ddot{\mathbf{x}}\right) - L^*\left(\mathbf{x}, \dot{\mathbf{x}}, \ddot{\mathbf{x}}\right)\right] dt \tag{A.1}$$

In Eq. (A.1), and in the ensuing analysis, the Lagrangian functional of Eq. (15) is denoted as $L^*(\mathbf{x}, \dot{\mathbf{x}}, \ddot{\mathbf{x}})$ for notation simplicity, where $\mathbf{x} = [x(t), \mathbf{u}_y^T]^T$. Next, applying Taylor's formula, the integrand in Eq. (A.1) is written as

$$\begin{aligned} &L^*\left(\mathbf{x}+\delta\mathbf{x}, \dot{\mathbf{x}}+\delta\dot{\mathbf{x}}, \ddot{\mathbf{x}}+\delta\ddot{\mathbf{x}}\right) - L^*\left(\mathbf{x}, \dot{\mathbf{x}}, \ddot{\mathbf{x}}\right) \\ &= \sum_{j=1}^{n+1} \left(\frac{\partial}{\partial x_j} L^* \delta x_j + \frac{\partial}{\partial \dot{x}_j} L^* \delta \dot{x}_j + \frac{\partial}{\partial \ddot{x}_j} L^* \delta \ddot{x}_j \right) + R_l \end{aligned} \tag{A.2}$$

where x_j represents the j-th component of the vector $\mathbf{x} = [x(t), \mathbf{u}_y^T]^T$, and R_l denotes an infinitesimal of higher order than $\delta x_j, \delta\dot{x}_j, \delta\ddot{x}_j$. Further, utilizing Eq. (A.2) and ignoring R_l, Eq. (A.1) becomes

$$\delta J^* = \sum_{j=1}^{n+1} \int_{t_i}^{t_f} \left(\frac{\partial}{\partial x_j} L^* \delta x_j + \frac{\partial}{\partial \dot{x}_j} L^* \delta \dot{x}_j + \frac{\partial}{\partial \ddot{x}_j} L^* \delta \ddot{x}_j \right) dt \tag{A.3}$$

Furthermore, integrating by parts the second and third terms in Eq. (A.3) yields

$$\begin{aligned} \int_{t_i}^{t_f} \frac{\partial}{\partial \dot{x}_j} L^* \delta \dot{x}_j dt &= \left[\frac{\partial}{\partial \dot{x}_j} L^* \delta x_j \right]_{t_i}^{t_f} - \int_{t_i}^{t_f} \frac{d}{dt} \frac{\partial}{\partial \dot{x}_j} L^* \delta x_j dt, \\ \int_{t_i}^{t_f} \frac{\partial}{\partial \ddot{x}_j} L^* \delta \ddot{x}_j dt &= \left[\frac{\partial}{\partial \ddot{x}_j} L^* \delta \dot{x}_j \right]_{t_i}^{t_f} - \left[\frac{d}{dt} \frac{\partial}{\partial \ddot{x}_j} L^* \delta x_j \right]_{t_i}^{t_f} \\ &\quad + \int_{t_i}^{t_f} \frac{d^2}{dt^2} \frac{\partial}{\partial \ddot{x}_j} L^* \delta x_j dt \end{aligned} \tag{A.4}$$

Next, substituting Eq. (A.4) into Eq. (A.3), the necessary condition of Eq. (22) for the minimization of the functional $J^*(\mathbf{x})$ becomes

$$\begin{aligned} \delta J^* = \sum_{j=1}^{n+1} \Bigg\{ &\int_{t_i}^{t_f} \left(\frac{\partial}{\partial x_j} L^* - \frac{d}{dt} \frac{\partial}{\partial \dot{x}_j} L^* + \frac{d^2}{dt^2} \frac{\partial}{\partial \ddot{x}_j} L^* \right) \delta x_j dt \\ &+ \left[\frac{\partial}{\partial \dot{x}_j} L^* \delta x_j \right]_{t_i}^{t_f} + \left[\frac{\partial}{\partial \ddot{x}_j} L^* \delta \dot{x}_j \right]_{t_i}^{t_f} - \left[\frac{d}{dt} \frac{\partial}{\partial \ddot{x}_j} L^* \delta x_j \right]_{t_i}^{t_f} \Bigg\} = 0 \end{aligned} \tag{A.5}$$

Note that for fixed boundary conditions at t_i and t_f the variations $\delta\mathbf{x}, \delta\dot{\mathbf{x}}, \delta\ddot{\mathbf{x}}$ become zero, and thus, Eq. (A.5) yields the Euler–Lagrange Eq. (23). Alternatively, consider the fixed boundary conditions

$$\begin{aligned} &x_1(t_i) = x_i, \dot{x}_1(t_i) = \dot{x}_i, x_1(t_f) = x_f, \dot{x}_1(t_f) = \dot{x}_f \\ &x_j(t_i) = 0, \dot{x}_j(t_i) = 0, j = 2, 3, \dots, n+1 \end{aligned} \tag{A.6}$$

whereas $x_j(t_f), \dot{x}_j(t_f), j = 2, 3, \dots, n+1$ are considered free. In this case, the variations $\delta\mathbf{x}, \delta\dot{\mathbf{x}}, \delta\ddot{\mathbf{x}}$ take the form

$$\begin{aligned} &\left[\delta x_j\right]_{t=t_i} = \left[\delta \dot{x}_j\right]_{t=t_i} = 0, j = 1, 2, \dots, n+1 \\ &\left[\delta x_1\right]_{t=t_f} = \left[\delta \dot{x}_1\right]_{t=t_f} = 0 \\ &\left[\delta x_j\right]_{t=t_f} = \delta x_{j,f}, \left[\delta \dot{x}_j\right]_{t=t_f} = \delta \dot{x}_{j,f}, j = 2, 3, \dots, n+1 \end{aligned} \tag{A.7}$$

As remarked previously, the most probable path $\mathbf{x}_c$ is also an extremal with respect to the more restricted class of functions $\mathbf{x}$ that have their boundaries fixed. In this regard, $\mathbf{x}_c$ also satisfies the Euler–Lagrange Eq. (23). Thus, the first term in Eq. (A.5) vanishes. Lastly, considering Eq. (A.5) in conjunction with the mixed fixed/free boundary conditions of Eq. (A.7) yields Eqs. (24)–(26); see also [41] for a broader perspective.

References

[1] Y.K. Lin, Probabilistic Theory of Structural Dynamics, McGraw-Hill, 1967.
[2] J.B. Roberts, P.D. Spanos, Random Vibration and Statistical Linearization, Dover, New York, 2003.
[3] R.G. Ghanem, P.D. Spanos, Stochastic Finite Elements: A Spectral Approach, Dover, New York, 2003.
[4] J. Li, J. Chen, Stochastic Dynamics of Structures, John Wiley & Sons, 2009.
[5] M. Grigoriu, Stochastic Systems: Uncertainty Quantification and Propagation, Springer Science & Business Media, 2012.
[6] M. Di Paola, G. Alotta, Path integral methods for the probabilistic analysis of nonlinear systems under a white-noise process, ASCE-ASME J. Risk Uncert Engrg. Syst. B Mech. Engrg. 6 (4) (2020).
[7] I.A. Kougioumtzoglou, I. Petromichelakis, A.F. Psaros, Sparse representations and compressive sampling approaches in engineering mechanics: A review of theoretical concepts and diverse applications, Probab. Eng. Mech. 61 (2020) 103082.
[8] N. Wiener, The average of an analytic functional, Proc. Natl. Acad. Sci. USA 7 (9) (1921) 253.
[9] M. Chaichian, A. Demichev, Path Integrals in Physics: Volume I Stochastic Processes and Quantum Mechanics, CRC Press, 2001.
[10] I.A. Kougioumtzoglou, A Wiener path integral solution treatment and effective material properties of a class of one-dimensional stochastic mechanics problems, J. Eng. Mech. 143 (6) (2017) 04017014.
[11] I. Petromichelakis, R.M. Bosse, I.A. Kougioumtzoglou, A.T. Beck, Wiener path integral most probable path determination: A computational algebraic geometry solution treatment, Mech. Syst. Signal Process. 153 (2021) 107534.
[12] I.A. Kougioumtzoglou, P.D. Spanos, An analytical Wiener path integral technique for non-stationary response determination of nonlinear oscillators, Probab. Eng. Mech. 28 (2012) 125–131.
[13] A.F. Psaros, O. Brudastova, G. Malara, I.A. Kougioumtzoglou, Wiener Path Integral based response determination of nonlinear systems subject to non-white, non-Gaussian, and non-stationary stochastic excitation, J. Sound Vib. 433 (2018) 314–333.
[14] I. Petromichelakis, A.F. Psaros, I.A. Kougioumtzoglou, Stochastic response determination of nonlinear structural systems with singular diffusion matrices: A Wiener path integral variational formulation with constraints, Probab. Eng. Mech. 60 (2020) 103044.
[15] A.F. Psaros, I.A. Kougioumtzoglou, I. Petromichelakis, Sparse representations and compressive sampling for enhancing the computational efficiency of the Wiener path integral technique, Mech. Syst. Signal Process. 111 (2018) 87–101.
[16] Y. Zhang, I.A. Kougioumtzoglou, F. Kong, Exploiting expansion basis sparsity for efficient stochastic response determination of nonlinear systems via the Wiener path integral technique, Nonlinear Dynam. 107 (2022) 3669–3682.
[17] I. Petromichelakis, I.A. Kougioumtzoglou, Addressing the curse of dimensionality in stochastic dynamics: a Wiener path integral variational formulation with free boundaries, Proc. R. Soc. Lond. Ser. A Math. Phys. Eng. Sci. 476 (2020) 20200385.
[18] P.D. Spanos, F. Kong, J. Li, I.A. Kougioumtzoglou, Harmonic wavelets based excitation–response relationships for linear systems: A critical perspective, Probab. Eng. Mech. 44 (2016) 163–173.
[19] I.A. Kougioumtzoglou, P.D. Spanos, Harmonic wavelets based response evolutionary power spectrum determination of linear and non-linear oscillators with fractional derivative elements, Int. J. Non-Linear Mech. 80 (2016) 66–75.

[20] A. Pirrotta, I.A. Kougioumtzoglou, A. Di Matteo, V.C. Fragkoulis, A.A. Pantelous, C. Adam, Deterministic and random vibration of linear systems with singular parameter matrices and fractional derivative terms, J. Eng. Mech. 147 (6) (2021) 04021031.
[21] K. Oldham, J. Spanier, The Fractional Calculus Theory and Applications of Differentiation and Integration to Arbitrary Order, Vol. 111, Academic Press, New York, 1974.
[22] J. Sabatier, O.P. Agrawal, J.A.T. Machado (Eds.), Advances in Fractional Calculus: Theoretical Developments and Applications in Physics and Engineering, Springer Netherlands, 2007.
[23] Y.A. Rossikhin, M.V. Shitikova, Application of fractional calculus for dynamic problems of solid mechanics: novel trends and recent results, Appl. Mech. Rev. 63 (1) (2010) 010801.
[24] M. Di Paola, G. Failla, A. Pirrotta, A. Sofi, M. Zingales, The mechanically based non-local elasticity: an overview of main results and future challenges, Phil. Trans. R. Soc. A 371 (1993) (2013) 20120433.
[25] V.E. Tarasov, Fractional mechanics of elastic solids: continuum aspects, J. Eng. Mech. 143 (5) (2017) D4016001.
[26] M. Di Paola, A. Pirrotta, A. Valenza, Visco-elastic behavior through fractional calculus: an easier method for best fitting experimental results, Mech. Mater. 43 (12) (2011) 799–806.
[27] P.D. Spanos, G.I. Evangelatos, Response of a non-linear system with restoring forces governed by fractional derivatives—Time domain simulation and statistical linearization solution, Soil Dyn. Earthq. Eng. 30 (9) (2010) 811–821.
[28] L. Chen, W. Zhu, First passage failure of SDOF nonlinear oscillator with lightly fractional derivative damping under real noise excitations, Probab. Eng. Mech. 26 (2) (2011) 208–214.
[29] P.D. Spanos, I.A. Kougioumtzoglou, K.R. dos Santos, A.T. Beck, Stochastic averaging of nonlinear oscillators: Hilbert transform perspective, J. Eng. Mech. 144 (2) (2018) 04017173.
[30] V.C. Fragkoulis, I.A. Kougioumtzoglou, A.A. Pantelous, M. Beer, Non-stationary response statistics of nonlinear oscillators with fractional derivative elements under evolutionary stochastic excitation, Nonlinear Dynam. 97 (4) (2019) 2291–2303.
[31] A. Di Matteo, I.A. Kougioumtzoglou, A. Pirrotta, P.D. Spanos, M. Di Paola, Stochastic response determination of nonlinear oscillators with fractional derivatives elements via the Wiener path integral, Probab. Eng. Mech. 38 (2014) 127–135.
[32] M. Di Paola, G. Failla, A. Pirrotta, Stationary and non-stationary stochastic response of linear fractional viscoelastic systems, Probab. Eng. Mech. 28 (4) (2012) 85–90.
[33] R. Haiwu, X. Wei, M. Guang, F. Tong, Response of a Duffing oscillator to combined deterministic harmonic and random excitation, J. Sound Vib. 242 (2) (2001) 362–368.
[34] N.D. Anh, N.N. Hieu, The Duffing oscillator under combined periodic and random excitations, Probab. Eng. Mech. 30 (2012) 27–36.
[35] P.D. Spanos, Y. Zhang, F. Kong, Formulation of statistical linearization for MDOF systems subject to combined periodic and stochastic excitations, J. Appl. Mech. 86 (10) (2019) 101003.
[36] P.D. Spanos, G. Malara, Nonlinear vibrations of beams and plates with fractional derivative elements subject to combined harmonic and random excitations, Probab. Eng. Mech. 59 (2020) 103043.
[37] L. Yuan, O.P. Agrawal, A numerical scheme for dynamic systems containing fractional derivatives, J. Vib. Acoust. 124 (2) (2002) 321–324.
[38] I. Petromichelakis, A.F. Psaros, I.A. Kougioumtzoglou, Stochastic response determination and optimization of a class of nonlinear electromechanical energy harvesters: A Wiener path integral approach, Probab. Eng. Mech. 53 (2018) 116–125.
[39] I. Petromichelakis, A.F. Psaros, I.A. Kougioumtzoglou, Stochastic response analysis and reliability-based design optimization of nonlinear electromechanical energy harvesters with fractional derivative elements, ASCE-ASME J. Risk Uncert Engrg. Syst. B Mech. Engrg. 7 (1) (2021) 010901.
[40] A.F. Psaros, Y. Zhao, I.A. Kougioumtzoglou, An exact closed-form solution for linear multi-degree-of-freedom systems under Gaussian white noise via the Wiener path integral technique, Probab. Eng. Mech. 60 (2020) 103040.
[41] C. Lanczos, The Variational Principles of Mechanics, Dover Publications, 1986.
[42] G.M. Ewing, Calculus of Variations with Applications, Dover Publications, Mineola, NY, 1985.
[43] J. Nocedal, S. Wright, Springer series in operations research and financial engineering, in: Numerical Optimization, Springer, New York, 2006.
[44] C.G. Koh, J.M. Kelly, Application of fractional derivatives to seismic analysis of base-isolated models, Earthq. Eng. Struct. Dyn. 19 (2) (1990) 229–241.
[45] M. Dimentberg, D. Iourtchenko, Random vibrations with impacts: a review, Nonlinear Dynam. 36 (2) (2004) 229–254.